

Performance Comparison of Various Labyrinth Side Weirs

¹R. J. Desai , Dr. L. G. Patil²

¹M.Tech Student, Department of Civil and Water Management Engineering, SGGSI&T, Nanded.

²Associate Professor, Department of Civil and Water Management Engineering, SGGSI&T, Nanded.

ABSTRACT

Side weirs are used generally to divert flows from rivers, canals, sewers and reservoirs. There are many studies focused on triangular and rectangular side weirs situated on a straight channel. Some recent studies exist on labyrinth side weirs. In this study various labyrinth weir shapes are compared for coefficient of discharge and surface profiles. The study aims at finding out performance of the labyrinth side weirs using computational fluid dynamics. It is found that for subcritical flow in parent channel, surface profiles along the centerline shows no fall at the beginning of the weir and shows increase in depth along the length of weir opening. The performance of parabolic and triangular shape with included angle 60° was found to be almost similar.

Keywords:Labyrinth Side Weir, CFD, Free Surface Flow

1. INTRODUCTION

Weirs are widely used in many different forms to regulate and measure the flow of water. Side weirs are used to divert flows from a main channel into a side channel when water level in main channel exceeds a specified limit. Labyrinth side weir is a side weir folded in plan view to increase the effective length of the weir resulting in more discharging capacity. Before discussing labyrinth side weirs it is necessary to understand characteristics of flow over a side weir. Flow over a side weir is a case of spatially varied flow with decreasing discharge. The governing equation for such type of flow is [1]-

$$\frac{dy}{dx} = \frac{S_0 - S_f - \frac{Q}{gA^2} \frac{dQ}{dx}}{1 - \frac{Q^2 T}{gA^3}} \quad (1)$$

Where S_0 represents bed slope of the channel, S_f is friction in terms of slope, Q is discharge in parent channel, g is the gravitational acceleration, A is cross sectional area of the flow, dQ represents partial outflow through the width dx along the side weir and T is top width of the flow. According to this equation, for subcritical flow the level of water rises along the side weir.

Considering an elementary strip of length ds along the side weir, the discharge dQ through it in a rectangular main channel in terms of De Marchi's equation is [2]-

$$q = -\frac{dQ}{ds} = \frac{2}{3} C_d \sqrt{2g} (h - p)^{3/2} \quad (2)$$

Q is the discharge in the main channel, s is the distance from start of the side weir, dQ/ds is the discharge per unit length of the side weir, g is gravitational acceleration, h is depth of flow at section s , $(h - p)$ is the pressure head over the weir and C_d is the discharge coefficient. So, $Q_s = qL$, where Q_s is total discharge over side weir. C_d depends on following parameters [3]-

$$C_d = f_1 \left(F_1, \frac{L}{b}, \frac{L}{h_1}, \frac{P}{h_1}, \psi, S_0 \right) \quad (3)$$

Here F_1 is the upstream Froude number, L is length of the side weir opening, b is the channel width, h_1 is the depth of water measured at the upstream end of the side weir along the centerline. ψ is the deviation angle of the flow and S_0 is the channel slope.

Hager [4] (1987) studied lateral outflow over side weirs and developed equations for Froude Number > 0 . Kumar and Pathak [5] (1987) have studied discharge characteristics of sharp and broad crested triangular side weirs experimentally. Uyumaz and Smith [6] (1991) did numerical investigation for design procedure of flow over side weir.

Swamee et al. [7] (1994) carried out experiments and proved an equation for elementary discharge coefficient. Singh et al. [8] (1994), Borghei et al. [9] (1999) also presented equations for finding out discharge coefficient of side weir. Bagheri et al. [10], [11] (2014) have recent studies on sharp crested side weirs which discuss traditional weir equation and Domínguez's method.

Aydin and Emiroglu [12] (2013) discussed the flow patterns and discharging capacity of labyrinth side weirs using CFD. Aydin [13] (2012) carried out CFD study of labyrinth side weir and compared the results for various turbulence models, grid and with experimental results. This study mainly involves surface profile configurations. Emiroglu et al. [14] (2010) extensively studied different configurations of labyrinth weir experimentally for surface profile and variation of discharge coefficient with different flow parameters.

Purpose of this study is to compare various shapes of labyrinth side weirs and evaluate their performance in terms of coefficient of discharge and surface profiles using CFD.

2. GOVERNING EQUATIONS

The Navier-Stokes equations (4) - (6) are the basic governing equations for a viscous fluid. It is supplemented by the mass conservation equation (7)

$$\frac{\partial u}{\partial t} + \frac{1}{V_F} \left\{ uA_x \frac{\partial u}{\partial x} + vA_y \frac{\partial u}{\partial y} + wA_z \frac{\partial u}{\partial z} \right\} = -\frac{1}{\rho} \frac{\partial p}{\partial x} + G_x + f_x \quad (4)$$

$$\frac{\partial v}{\partial t} + \frac{1}{V_F} \left\{ uA_x \frac{\partial v}{\partial x} + vA_y \frac{\partial v}{\partial y} + wA_z \frac{\partial v}{\partial z} \right\} = -\frac{1}{\rho} \frac{\partial p}{\partial y} + G_y + f_y \quad (5)$$

$$\frac{\partial w}{\partial t} + \frac{1}{V_F} \left\{ uA_x \frac{\partial w}{\partial x} + vA_y \frac{\partial w}{\partial y} + wA_z \frac{\partial w}{\partial z} \right\} = -\frac{1}{\rho} \frac{\partial p}{\partial z} + G_z + f_z \quad (6)$$

$$\frac{\partial uA_x}{\partial x} + \frac{\partial vA_y}{\partial y} + \frac{\partial wA_z}{\partial z} = 0 \quad (7)$$

Where, V_F is the fractional volume open to flow, ρ is fluid density, (u, v, w) are velocities in (x, y, z) direction respectively, t is time, (A_x, A_y, A_z) are fractional areas open to flow in direction (x, y, z) . (G_x, G_y, G_z) are body accelerations, (f_x, f_y, f_z) are viscous accelerations. These are the simplified equations for incompressible free surface flow with constant viscosity.

Fluid configuration is defined in terms of volume of fluid (VOF) function, $F(x, y, z, t)$. This function represents the volume of fluid per unit volume and satisfies the equation (8).

$$\frac{\partial F}{\partial t} + \frac{1}{V_F} \left[\frac{\partial}{\partial x} (FA_x u) + \frac{\partial}{\partial y} (FA_y v) + \frac{\partial}{\partial z} (FA_z w) \right] = 0 \quad (8)$$

Navier-Stokes equations are solved by using readily available software. The Continuous domain is replaced by a discrete domain using a grid. For every cell of the grid the discrete equations are derived, boundary conditions are defined and solved. Though the solution can never be exact, it can be fairly accurate. Various numerical methods exist to solve the differential equations. Finite Volume method for solving the equations is used.

3. NUMERICAL MODEL

The geometries for the simulation were created using Autodesk Inventor. The geometry consists of certain necessary solid parts for efficient simulation. Side weir is placed half way down the channel. The labyrinth side weirs of various shapes, particularly triangular (90° and 60° included angle), Semicircular and Parabolic in plan were considered for numerical simulation. The side weir opening was kept constant and the above mentioned shapes of labyrinth side weir were fitted in the same side weir opening. The Semicircular labyrinth side weir dimension was chosen such that it circumscribes the 90° Triangular shape. Similarly the Parabolic shape circumscribes the 60° Triangular Shape. Excess portion around the side weir where water will not be present are blocked by solid to save computations. Main Channel is 0.5m wide and the side weir opening is 0.75m wide. Height of the side weir is 0.12m.

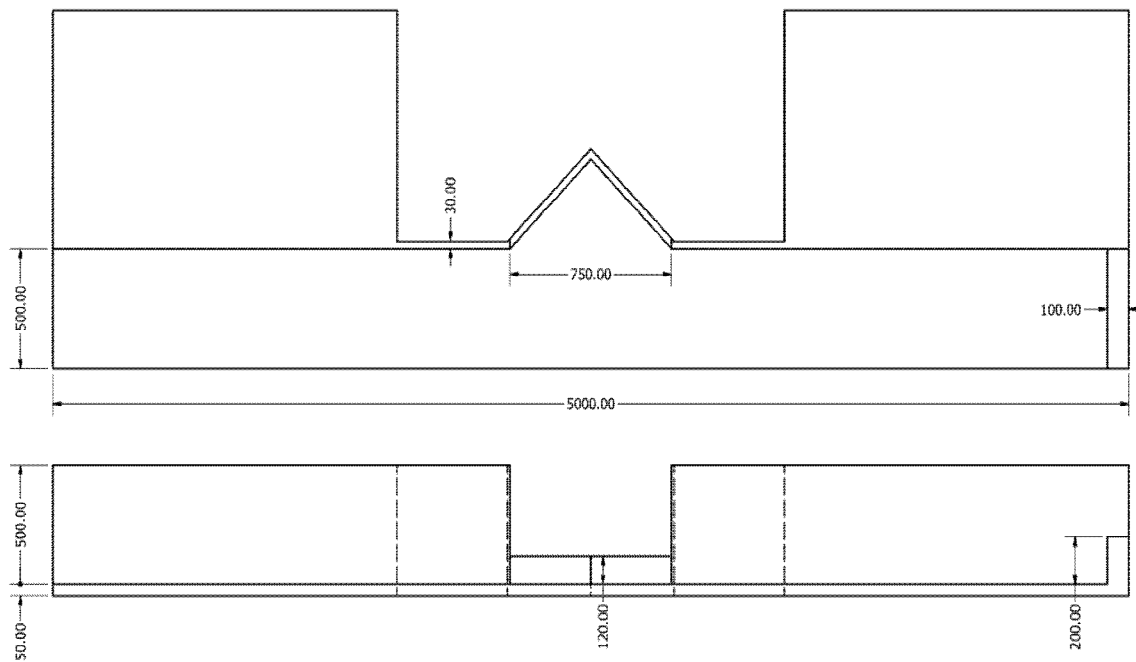


Figure 1: Plan and Elevation of Triangular labyrinth side weir with 90° included angle model with dimensions

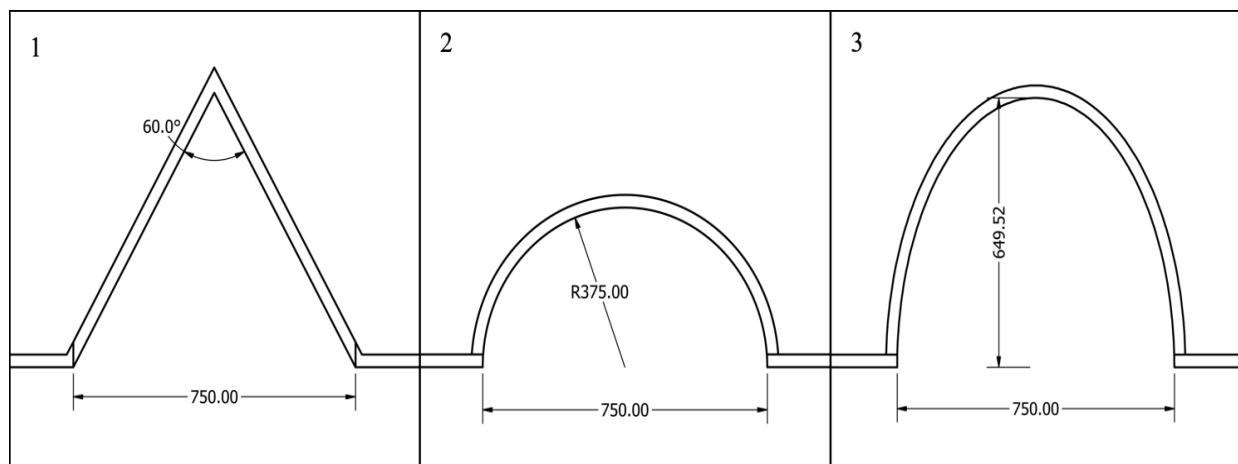


Figure 2: Labyrinth side weir shapes with dimensions - Triangular with included angle 60°(1), Semicircular(2),Parabolic(3)

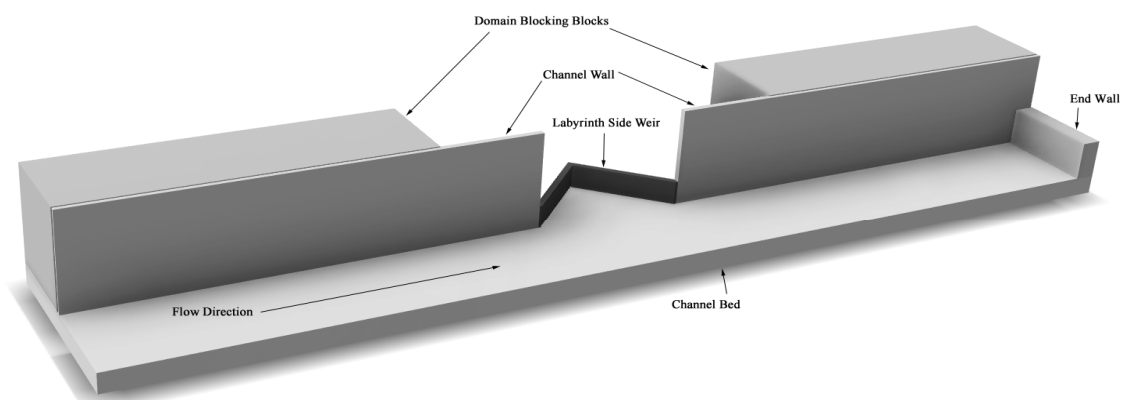


Figure 3: 3D representation of the model showing various parts

The software utilises structured hexahedral free mesh and an algorithm to represent solid obstacles in the domain. Cell size is kept as 0.014m, uniform in all directions, around 1 million cells were present in all the cases.

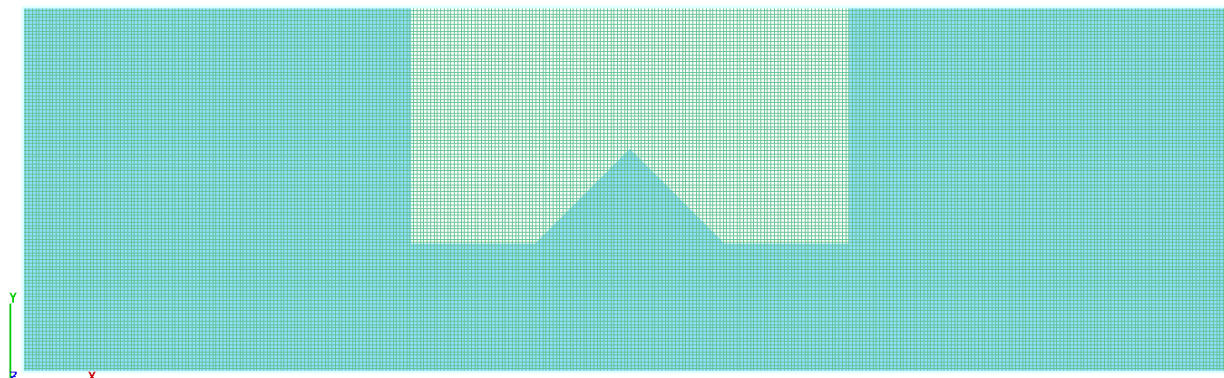


Figure 4: XY view of the meshed geometry

Flow over the side weir leaves the domain from bottom boundary of the side channel (hence no submergence of crest is expected) and discharge was measured at that boundary. Inlet was represented by ‘volume flow rate’ boundary condition for which discharge was specified. At the outlets ‘outflow’ boundary condition was selected. Two equation RNG turbulence model was chosen for solving the problem.

Total 20 cases were solved with discharges varying from 0.1 to 0.2 m³/s for each of four geometric configurations. Froude number was less than unity for all the cases (only subcritical flow in the parent channel was considered)

4. Results and Discussions

Discharge over the labyrinth side weir was measured and the coefficient of discharge was computed for total 20 cases using eq. (2). The coefficient of discharge and water surface profiles along the centerline for four labyrinth side weir shapes were compared.

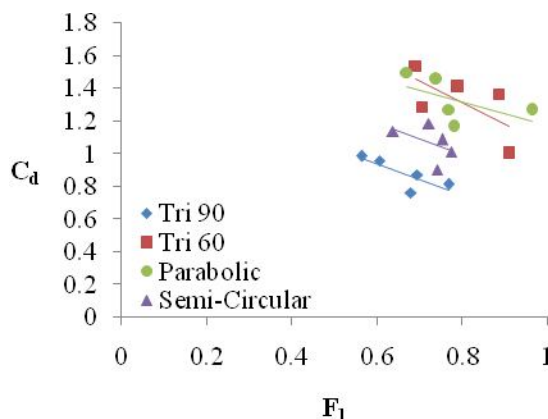


Figure 5: Comparison of Discharge Coefficients of various shapes of labyrinth side weirs

The plot of discharge coefficient versus Froude number is presented in fig. 5. Amongst all the shapes considered for the study, lowest C_d values were obtained for Triangular labyrinth side weir with included angle 90°. Triangular shape with 60° included angle and parabolic shape show almost same trend in variation of coefficient discharge. Even though the crest length of the parabolic shape is more than that of triangular shape, both cases show somewhat similar discharge coefficients, whereas the difference in C_d is more in triangular shapes and semi-circular shape. It can be said that the semi-circular shape has more discharging capacity than the triangular shape with 90° included angle, but less than that of the triangular labyrinth side weir with 60° included angle. For all the different shaped labyrinth side weirs, the coefficient of discharge is reducing with increasing Froude number.

Surface profiles for various shapes are compared at different discharges. In all the cases water level rises along the side weir. The rise in depth is not uniform. It can be seen that with increasing discharge the water depth also rises.

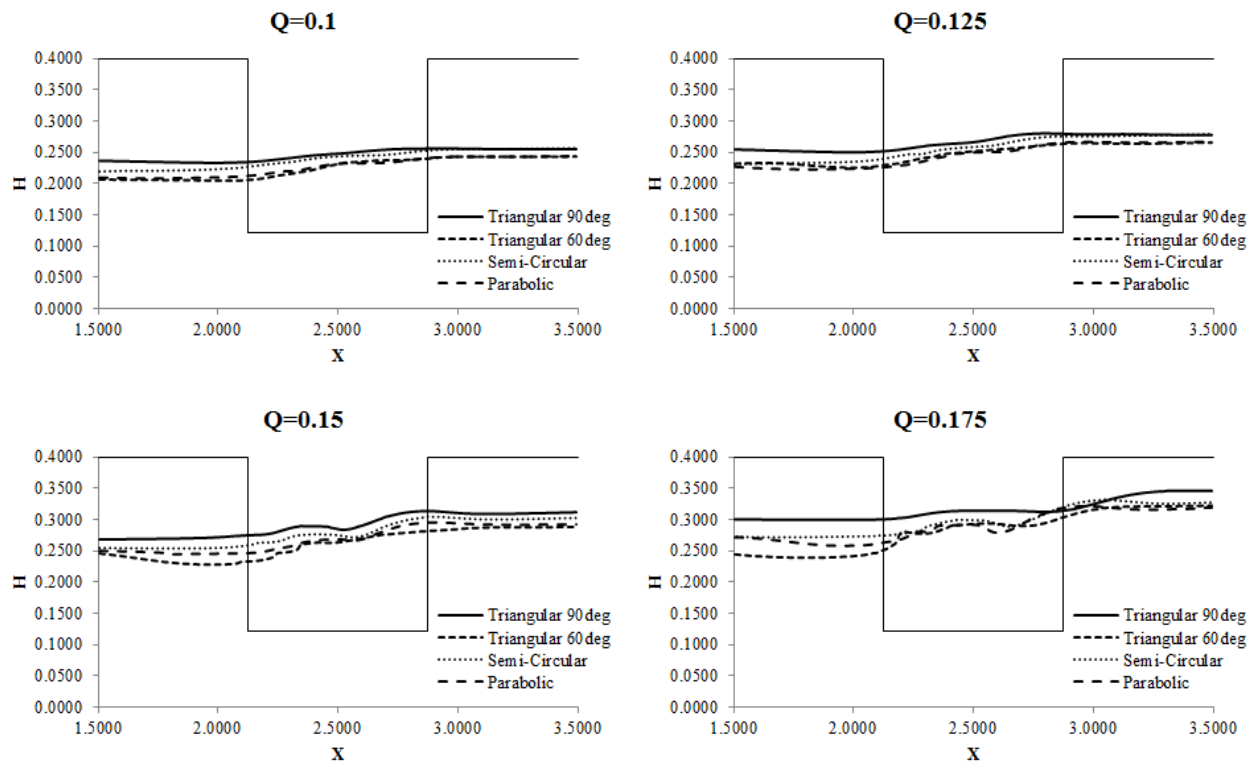


Figure 6: Variation of surface profile with different shapes of labyrinth side weirs at various discharges

It shows that parabolic and triangular shape with 60° included angle show almost overlapping surface profiles for discharges 0.1 and 0.125 m³/s. Depth of water in the parent channel is different for different shapes for the same discharge. Depth of water is highest in case of triangular shape with 90° included angle, followed by semi-circular and then lowest in cases of parabolic and triangular shape with 60° included angle.

5. CONCLUSION

Four shapes of labyrinth side weir are compared for discharges 0.1 to 0.2 m³/s. total 20 cases are solved and data is processed for obtaining surface profiles at the centerline of the parent channel and coefficient of discharge. From the results, following conclusions are made-

Water level before the labyrinth side weir is less than that of the water level after the labyrinth side weir. Depth of flow increases along the side weir opening. This increase in depth is not uniform and it is non-linear along the channel length. Irregularity in the depth is maybe due to existence of the eddy inside the labyrinth shape.

Coefficient of discharge decreases with increase in Froude number. This is due to increase in momentum at higher Froude numbers due to which it is difficult for the flow to turn and fall out over the side weir. Semi-circular labyrinth side weir shows better performance over triangular labyrinth side weir with 90° included angle; but same is not true about Parabolic and Triangular shape with 60° included angle. Both show similar coefficients of discharge.

References

- [1] C. M. Aydin, "CFD Simulation of Free-Surface Flow over Triangular Labyrinth Side Weir", *Advances in Engineering Software*, 45, pp.159–166, 2012
- [2] C. M. Aydin, M. E. Emiroglu, "Determination of Capacity of Labyrinth Side Weir by CFD", *Flow Measurement and Instrumentation*, 29, pp.1–8, 2013.
- [3] M. E. Emiroglu, N. Kaya, H. Agaccioglu, "Discharging Capacity of Rectangular Side Weirs in Straight Open Channels", *Flow Measurement and Instrumentation* 22, pp. 319–330, 2011.
- [4] W. H. Hager, "Lateral Outflow over Side Weirs", *Journal of Hydraulic Engineering*, Vol. 113, No. 4, pp. 491-504, 1987.
- [5] C. P. Kumar, S. K. Pathak, "Triangular Side Weirs", *Journal of Irrigation and Drainage Engineering*, Vol 113, No. 1, pp. 98-105, 1987.
- [6] A. Uyumaz, R. H. Smith, "Design Procedure for Flow over Side Weir", *Journal of Irrigation and Drainage Engineering*, Vol. 117, No. 1, pp. 79-90, 1991.

- [7] P. K. Swamee, S. K. Pathak, M. S. Ali, 1994, "Side Weir Analysis Using Elementary Discharge Coefficient", *Journal of Irrigation and Drainage Engineering*, Vol. 120, No. 4, pp. 742-755, 1994.
- [8] P. K. Swamee, S. K. Pathak, M. Mohan, S. K. Agrawal, M. S. Ali, "Subcritical Flow over Rectangular Side Weir", *Journal of Irrigation and Drainage Engineering*, Vol. 120, No. 1, pp. 212-217, 1994.
- [9] R. Singh, D. Manivannan, T. Satyanarayana, "Discharge Coefficient of Rectangular Side Weirs", *Journal of Irrigation and Drainage Engineering*, Vol. 120, No. 4, 814-819, 1994.
- [10] S. M. Borghei, M. R. Jalili, M. Ghodsian, "Discharge Coefficient for Sharp-Crested Side Weir in Subcritical Flow", *Journal of Hydraulic Engineering*, Vol. 125, No. 10, pp. 1051-1056, 1999.
- [11] S. Bagheri, A. R. Kabiri-Samani, M. Heidarpour, "Discharge coefficient of Rectangular Sharp-Crested Side Weirs, Part I: Traditional Weir Equation", *Flow Measurement and Instrumentation*, 35, pp. 109-115, 2014.
- [12] S. Bagheri, A. R. Kabiri-Samani, M. Heidarpour, "Discharge coefficient of Rectangular Sharp-Crested Side Weirs, Part I: Dominguez's Method", *Flow Measurement and Instrumentation*, 35, pp. 116-121, 2014.
- [13] M. E. Emiroglu, N. Kaya, H. Agaccioglu, "Discharge Capacity of Labyrinth Side Weir Located on a Straight Channel", *Journal of Irrigation and Drainage Engineering*, Vol. 136, No. 1, 37-46, 2010.
- [14] S. Bagheri, M. Heidarpour, "Characteristics of Flow over Rectangular Sharp-Crested Side Weirs", *Journal of Irrigation and Drainage Engineering*, Vol. 138, No. 6, pp. 541-547, 2012.